

Electrochemical determination of sulfur-containing amino acid on Screen–Printed Carbon Electrode modified with Graphene Oxide

Ragu Sasikumar¹, Palraj Ranganathan², Shen-Ming Chen^{1*}, Thavuduraj Kavitha³, Shih-Yi Lee⁴, Tse-Wei Chen¹, Wen-Han Chang^{5,6,7}

¹ Department of Chemical Engineering and Biotechnology, National Taipei University of Technology, No. 1, Section 3, Chung-Hsiao East Road, Taipei 106, Taiwan, ROC.

² Institute of Organic and Polymeric Materials, National Taipei University of Technology, No. 1, Section 3, Chung-Hsiao East Road, Taipei 106, Taiwan, ROC.

³ Department of Chemistry, Sri S. Ramasamy Naidu Memorial College, Sattur, Virudhunagar District, Tamil Nadu, India.

⁴ Division of Pulmonary and Critical Care Medicine, MacKay Memorial Hospital; MacKay Medicine, Nursing and Management College.

⁵ MacKay Memorial College Department of Cardiology, MacKay Memorial Hospital, Taiwan.

⁶ Department of Emergency Medicine, MacKay Memorial Hospital; Institute of Mechatronic Engineering, National Taipei University of Technology, Taiwan

⁷ Graduate Institute of Injury Prevention and Control, Taipei Medical University; Department of Medicine, Taiwan

*E-mail: smchen78@ms15.hinet.net

Received: 18 January 2017 / Accepted: 2 March 2017 / Published: 12 April 2017

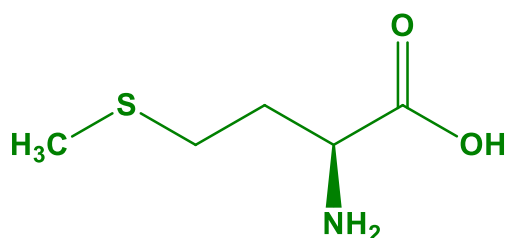
The current study discussed with sensitive L-Methionine (L-Met) sensor relative on a graphene oxide (GO) modified screen–printed carbon electrode (SPCE) was developed. The fabricated GO/SPCE displayed an enhanced current (I_{pa}) response towards L-Met relative to that of a bare SPCE. Under optimum conditions, the GO/SPCE showed a wide linear range at L-Met concentrations of 2-96 μM . The lower level of detection of 0.18 μM , and sensitivity of about 6.75 $\text{mA mM}^{-1}\text{cm}^{-2}$. The fabricated sensor displays good stability, reproducibility, and repeatability.

Keywords: Graphene oxide, L-Met, lecithin, screen–printed carbon electrode, differential pulse voltammetry.

1. INTRODUCTION

Newly, graphene oxide (GO) which was generally derived from exfoliation of graphite oxide [1], has involved great attraction owing to its layered structure of GO containing nanocomposites, and superior surface properties [2]. Exactly, GO shows good dispersibility in most of the solvents, especially in water medium [3] and ease of post-functionalization due to an introduction of rich oxygen-containing functional groups on the surface, like as hydroxyl, carbonyl, epoxy, and carboxyl groups. The functional groups act as announcer site and allow nanostructures attributing on the surface of GO sheets [4], forming different composites. These composites frequently possess rare properties when compared with their separate components and can be used as outstanding electrode materials [5,6]. Additionally, GO used in many fields, such as sensors [7], electronics [8], and energy storage [9,10] because of its excellent electro-catalytic and electronic properties.

Sulfur attached molecules are broadly circulated in animals, and plants and they show a vital role in the alive system [11]. Composed with L-methionine (L-Met), cysteine has two sulfur-containing proteinogenic amino acids. It founds and prevents the illnesses in skin, and hair. It is a significant amino acid through a central part for natural methylation reactions. L-Met used to reduce the cholesterol level, and increasing lecithin creation in a liver and also important for human growth [12]. Thiol imbalance has been associated with multiple disorders, ex. Alzheimer's, vascular disease, and cancer. Insufficiencies of L-Met have been accredited to depression, impaired growth, toxemia, and muscle paralysis [13]. Therefore, the detection of L-Met is quite significant in the medical point of view. The electrochemical technique has noteworthy responsiveness due to its tremendous selectivity, and sensitivity, simple procedure, price efficiency, and quick answer. Lots of electrochemical studies of L-Met have been reported by means of change of modified electrodes such as an electro-polymerized film of non-peripheral amine substituted Cu(II) phthalocyanine, glassy carbon electrode (GCE), graphene oxide/ α -cyclodextrin hybrid, and Boron doped diamond. The chemical structure of L-Met as displayed in Scheme 1.



Scheme 1. Chemical structure of L-Met.

Moreover, a better part of examining is mostly attentive on an electro-oxidation act of electrode properties rather than the sensitivity, and selectivity of L-Met determination [14-16]. Remarkably, the current study discussed about the preparation of GO, and the electrochemical oxidation of L-Met using the GO, and characterization of as-prepared GO by XRD, SEM, FT-IR, cyclic voltammetry, and differential pulse voltammetry analysis.

2. EXPERIMENTAL SECTION

2.1. Materials

Graphite flakes (~105 mm flakes), sodium nitrate (NaNO_3), potassium permanganate (KMnO_4), sulphuric acid (H_2SO_4), hydrogen peroxide (H_2O_2), hydrochloric acid (10% HCl) were purchased from Shanghai Chemical Reagent Co. L- Methionine ($\geq 98\%$) were got from Sigma-Aldrich, Taiwan (ROC). The electrochemical response of GO studied by cyclic voltammetry (CV), and differential pulse voltammetry (DPV) using CHI 400, and CHI 900 electrochemical analyzer (CH instruments). For electrochemical device studies, we have-used three electrode system, they are i) modified (GCE:surface area 0.0721 cm^2) working electrode, ii) reference electrode (saturated Ag/AgCl), and iii) counter electrode (Pt wire). For whole electrochemical experiments were carried out in N_2 saturated condition, the supporting electrolyte where in 0.05 M phosphate buffer which was prepared by mixture of Na_2HPO_4 , and NaH_2PO_4 . DI water was used whole experiments.

2.2. Methods

2.2.1. Preparation of GO

GO was prepared by the modified Hummers method [17]. Initially, 2 g of graphite flakes, and 2 g of sodium nitrate were mixed in 90 mL of sulphuric acid, and kept in an ice bath with constant stirring. Later, 12 g of potassium permanganate was added to the above mixture with very slowly. The mixture was diluted and kept in stirring for 2 h. Later, the ice bath was removed, and the mixture was stirred at $35 \text{ }^\circ\text{C}$ for 2 h, and reflux system at $98 \text{ }^\circ\text{C}$ for 10-15 min. After that the temperature to $30 \text{ }^\circ\text{C}$ to yield a pale brown colored solution. Finally, the solution was treated with 50 ml hydrogen peroxide the color changes brown to bright yellow. The resultant mixture is washed frequently using centrifugation with 10% hydrochloric acid, and then with DI water for 4-5 times up to it forms a jelly-like substance (pH 7). After centrifugation, the jelly-like substance is vacuum dried at $60 \text{ }^\circ\text{C}$ for overnight to get GO powder.

2.2.2. Fabrication of GO/SPCE

The prepared GO was firstly re-dispersed in water (0.01 mg mL^{-1}), and keep in ultra-sonication treatment for 60 min. On surface of SPCE, the optimized the concentration of about $8 \text{ } \mu\text{L}$ of a dispersed solution was drop cast on the energetic surface of the SPCE followed by dried in an air oven at $30 \text{ }^\circ\text{C}$ for 1 h.

2.2.3. Characterization

The crystalline arrangement of the GO was characterized by X-ray diffraction (XRD; XPERT-PRO) by (PANalytical B.V., The Netherlands) diffractometer (Cu $\text{K}\alpha$ radiation, $\lambda=1.54 \text{ \AA}$). Fourier-transform infrared (FT-IR; Bruker IFS28) spectrum was recorded with a spectral resolution of 2 cm^{-1}

using dry KBr pellet at room temperature. The surface morphology of the as-prepared GO was studied by field emission scanning electron microscopy (FE-SEM; Hitachi S-3000 H) at room temperature.

3. RESULTS AND DISCUSSION

X-Ray diffraction measurements were observed to examine the structure, and phase of the as-prepared GO. As shown in Fig. 1a, the X-Ray diffraction pattern of the as-synthesized GO shows a strong peak at $2\theta = 11.31^\circ$, equivalent to the (001) reflection of GO [18]. The FT-IR spectrum is given in Fig. 1b. For GO, the -OH symmetric stretching, and bending vibrations appeared at 3419, and 1633 cm^{-1} correspondingly due to absorbed water molecules. The minor absorption band of 1381 cm^{-1} and 1060 cm^{-1} represents -C=O and C-O vibration of -COOH located at GO sheet surface [19]. The SEM image of GO (Fig. 1c) obviously shows the typical crumpled layer structure. The GO nano-sheets folding composed and make a more accessible surface area. The higher surface area of GO provides good electrical conductivity.

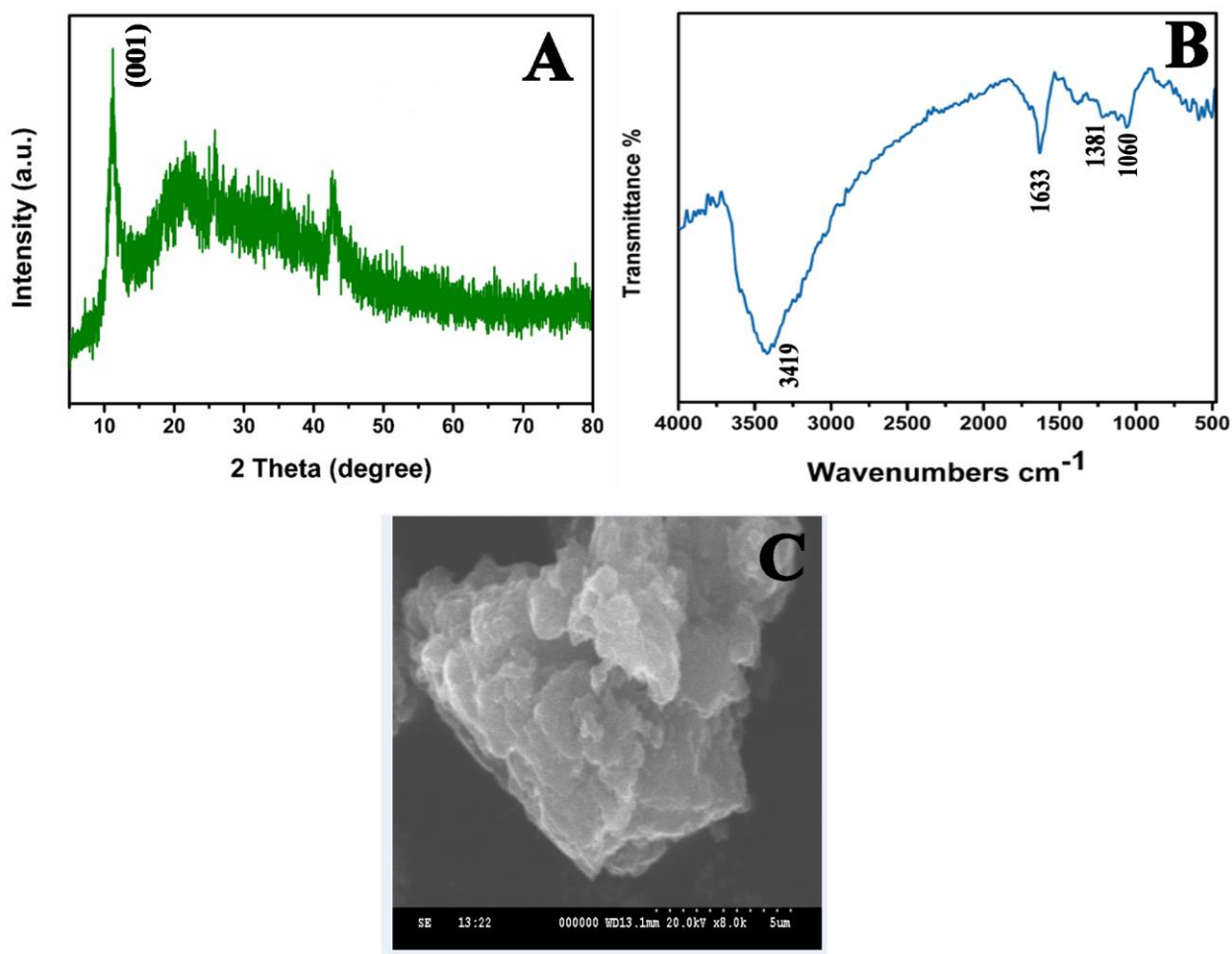
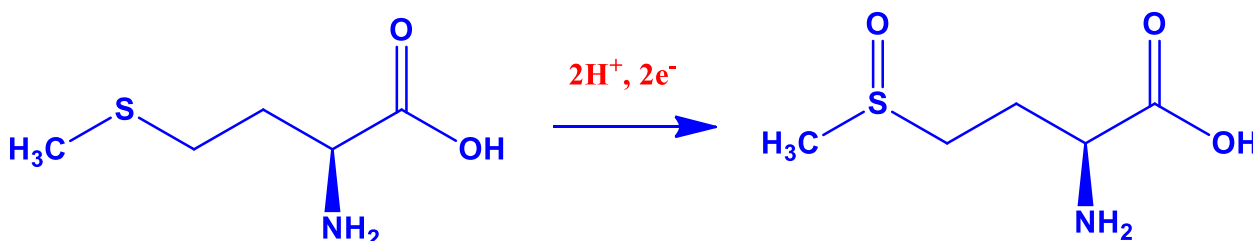


Figure 1. (A) X-Ray diffraction pattern, (B) FT-IR, and (C) SEM image of as-prepared GO.

3.1. Electro-oxidation of L-Met at GO/SPCE

The electro-oxidation activity of the bare SPCE and modified SPCE was observed by Cyclic Voltammetry (CVs). Fig. 2A displays the CV curves of various modified electrodes such as (a) bare SPCE absence of L-Met (b) bare SPCE presence of 200 μM L-Met, and (c) GO/SPCE with 200 μM of L-Met in (pH 7) PBS at the scanning rate of 50 mV s^{-1} . There is no visible peak appeared while introduced SPCE into the electrochemical arrangement. In the adding of L-Met in bare SPCE a shows small difference in the CV curve with a small peak potential (1.374 V) at E_{pa} (anodic peak potential) with a small current. The well-marked anodic peak potential (E_{pa}) were detected at 1.200 V for the GO/SPCE as shown in Fig. 2A. The results show that the electrochemical behavior of L-Met has an irreversible, and oxidation-oxidation process. However relatively, GO/SPCE is displayed supreme electro-oxidation performance associated to bare SPCE in terms of less over potential with high peak currents. Therefore, GO/SPCE takes a greater electro-oxidation ability to the oxidation of L-Met due to the perfect synergy amongst high conductivity, and big surface area of the excellent electro-oxidation capability of GO. The large anodic peaks happen at peak potentials of 1.200 V due to $2e^-$ oxidation of the L-Met. The L-Met molecules were fascinated by the modified electrode and are oxidized at 1.200 V. The CV curves definitely authorizes that the GO/SPCE is an excellent electrochemical determination of L-Met. From the literature survey we understood that the respective electrochemical reaction of L-Met is an irreversible oxidation reaction involving with two electrons, and two protons as given in the mechanism in Scheme 2 [16].



Scheme 2. Oxidation mechanism of L-Met.

3.2. Effect of concentrations and scan rates

Fig. 2B shows CV responses of GO/SPCE in PBS containing various additions of L-Met at a scanning rate of 50 mVs^{-1} . When the absence of L-Met (a), the GO/SPCE does not show any discernible peaks; whereas a definite oxidation peak was detected in the presence of 100 μM of L-Met. Additionally, the oxidation peaks current of the L-Met increases with increasing the concentrations from 100 to 700 μM of L-Met (b-h). The results reveals that the excellent electro-oxidation behavior of L-Met at GO/SPCE and can be used for sensitive determination of L-Met.

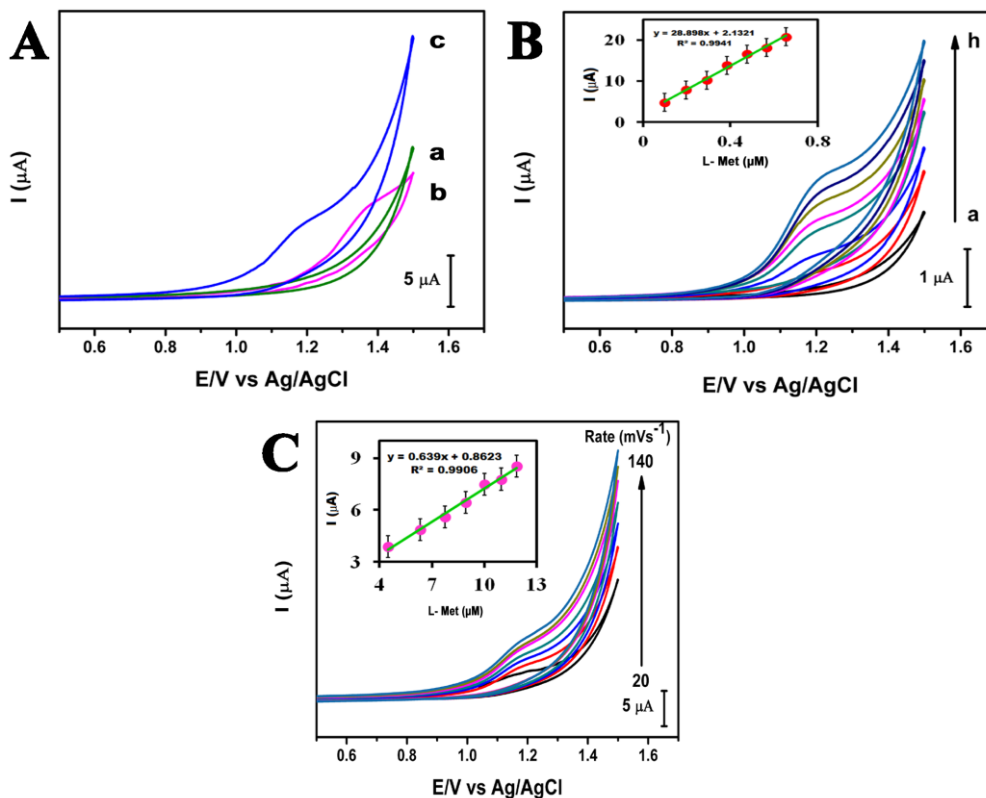


Figure 2. (A) CVs of (a) bare SPCE absence of L-Met (b) bare SPCE with 200 μM L-Met (c) GO/SPCE with 200 μM L-Met in 0.05 M PBS (pH 7), (B) Various additions of L-Met at a scan rate of 50 mV s⁻¹, and (C) Various scan rates from 20 to 140 mV s⁻¹ (inset) plot of oxidation peak current versus the square root of the scan rates.

Fig. 2C shows that the effect of scanning rate of electro-oxidation responses of GO/SPCE in PBS (pH 7) for the detection of L-Met. The CV curves observed the oxidation peaks currents are gradually increased when increasing the anodic peaks from 20 to 140 mVs⁻¹. When the oxidation peaks current (I_{pa}) increases the scan rate also increases linearly. Additionally, the inset linear plot among oxidation peak current versus the square root of the scan rates has displayed a relationship which suggesting that the oxidation process of L-Met appeared at the GO/SPCE is a diffusion controlled electron relocation process (inset Fig. 2C). From the results, we approve that the observed CV reports are owing to the determination of L-Met diffused on the surface of the GO/SPCE. The inset in Fig. 2C demonstrates the plot between oxidation peak current, and the square root of scan rate, which may be communicated by a linear regression equation as $E_{pa} (V) = 0.639x - 0.8623$, $R^2 = 0.9906$. The above results are clearly confirming that the process is a diffusion controlled irreversible process [20].

$$LOD = 3S_b/b \quad \text{-----} 1$$

The LOD is calculated by using the above formula, slope of the straight line of the electrochemical analytical curve, and SD of the mean value for seven voltammograms of the blank (S_b).

3.3. Electrochemical oxidation of L-Met

The electrochemical oxidation of L-Met was completed at GO/SPCE by DPV. The DPV technique is a more sensitive method for the detection of L-Met than CV. The DPV responses of the GO/SPCE with the additions of various concentration of L-Met (2-96 μM) into the PBS (pH 7).

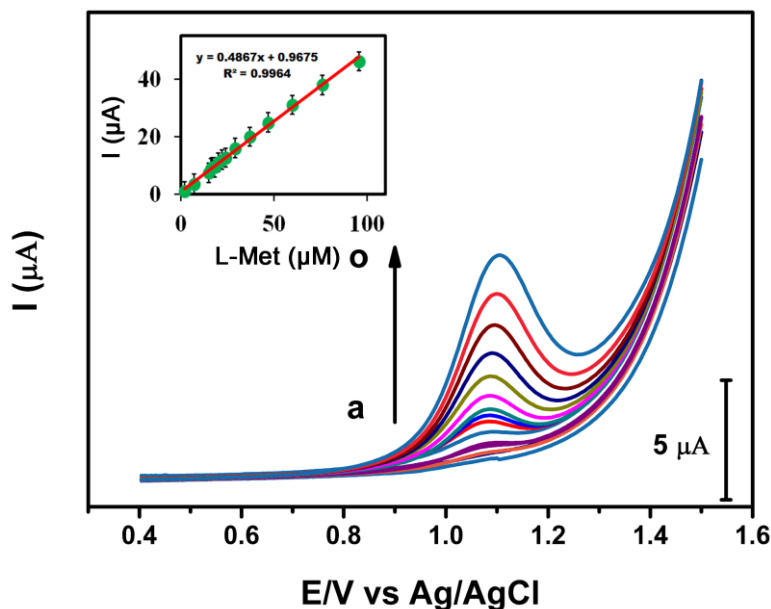


Figure 3. DPVs of increasing L-Met concentration (a to o = 2-96 μM) (inset) calibration curve of the peak currents on the L-Met concentrations.

The sensitivity was calculated by using the slope of the calibration plot [21] as shown in the inset of Fig. 3. The calculated sensitivity was about $6.750 (\pm 0.002) \mu\text{A} \mu\text{M}^{-1} \text{cm}^{-2}$, and limit of detection (LOD) is $0.184 \mu\text{M}$. A linear relationship between L-Met concentration vs peak current (I_{pa}) was obtained using 2-96 μM of L-Met, and a linear regression values, and correlation coefficient as $I_{\text{pa}} (\text{V}) = 0.4867x + 0.9675$ and $R^2 = 0.9964$ respectively. The detection limit was $0.184 \mu\text{M}$ observed from the slope of the calibration plot, as shown in the inset in Fig. 3.

3.4. Stability, reproducibility, and repeatability

In order to examine storing stability of the GO/SPCE, its electro-catalytic answer towards L-Met ($100 \mu\text{M}$) is checked up to one week of the storage period, the catalytic current slightly decreased, while 93.32% of the initial response current was engaged which exposes good storing stability of the film. Additionally, the electrode displays considerable repeatability with relative standard deviation (RSD) of 3.65% for five repetitive measurements carried out using single electrode and it displays considerable reproducibility with RSD of 3.26% for five self-determining measurements carried out in five different electrodes.

Similarity of analytical parameters such as linear range, and limit of detection for the various modified electrodes performance in the detection of L-Met.

Table 1. Similarity parameters for detection of L-Met at a various modified electrode.

Electrode Substrate	Linear range (M)	Detection limit (M)	Ref
ETAP-Cu(II)/GCE	$5.0 \times 10^{-5} - 5.0 \times 10^{-4}$	2.7×10^{-8}	22
PAMT/GCE	$1.0 \times 10^{-7} - 1.0 \times 10^{-4}$	4.1×10^{-10}	23
Au-Cys/GCE	$1.0 \times 10^{-6} - 1.0 \times 10^{-4}$	5.9×10^{-7}	24
PMV/Pt	–	1.0×10^{-3}	25
Ru ^{II} Den/CE	$1.0 \times 10^{-6} - 1.0 \times 10^{-5}$	6.0×10^{-7}	26
Bi(V)-PbO ₂ /Au	–	1.0×10^{-3}	27
Ni/CCE	$2.0 \times 10^{-6} - 9.0 \times 10^{-5}$	2.0×10^{-6}	28
Rh ₂ POM/CE	–	7.3×10^{-4}	29
SWCNT-NiCNT/GCE	$1.0 \times 10^{-5} - 1.0 \times 10^{-4}$	4.5×10^{-6}	30
Co(OH) ₂ /GCE	$2.5 \times 10^{-1} - 1.2 \times 10^0$	1.6×10^{-4}	31
F-C60/GCE	$1.0 \times 10^{-5} - 1.0 \times 10^{-3}$	8.2×10^{-6}	32
GO/SPCE	$2.0 \times 10^{-6} - 9.6 \times 10^{-5}$	1.8×10^{-7}	This work

ETAP-Cu(II) = Electropolymerized film 1,8,15,22-tetraaminophthalocyanato-Cu(II), PAMT = Poly (3-amino-5-mercapto-1,2,4-triazole), Au-Cys = Colloidal-gold cysteamine, PMV = Poly (methyl violet), Pt = Platinum, CPE = Carbon paste electrode, Ru^{II} Den = Ruthinium(II) dendrimer, CE = Carbon-composite electrode, Bi(V)-PbO₂ = Bi(V) doped PbO₂ film, CCE = Carbon ceramic electrode, SWCNT-NiCNT = Single-wall carbon nanotube and nickel-carbon nanotube, Co(OH)₂ = Cobalt hydroxide, Full-C60 = Fullerene-C60, GO = Graphene Oxide, SPCE = Screen printed carbon electrode.

4. CONCLUSIONS

In conclusion, GO was prepared by a modified Hummers method. The as-prepared GO was characterized by X-ray diffraction (XRD), field emission scanning electron microscopy (FE-SEM), Fourier-transform infrared (FT-IR) spectra which showed that the sheet-like structure. The as-prepared GO has high dispersible property in water. The modified SPCE of GO have electro-oxidation action towards the determination of L-Met. The electrochemical performance of the GO/GCE were observed using cyclic voltammetry (CV) and differential pulse voltammetry (DPV). From the electrochemical study, the limit of detection, sensitivity, and linear range are 0.18 μM , 6.750 (± 0.002) $\mu\text{A } \mu\text{M}^{-1} \text{cm}^{-2}$, and 2-96 μM . The fabricated sensor showed a remarkable electro-oxidation performance with a good sensitivity property and low limit of detection.

ACKNOWLEDGEMENT

This project was supported by the National Science Council and Ministry of Education, Taiwan (Republic of China).

References

1. R. Ruoff, *Nat. Nanotechnol.*, 3 (2008) 10.
2. S. K. Srivastava and J. Pionteck, *J. Nanosci. Nanotechnol.*, 15 (2015) 1984.
3. M. Seredych and T. J. Bandosz, *Carbon* 45 (2007) 2130.
4. M. Khan, M. N. Tahir, S. F. Adil, H. U. Khan, M. R. H. Siddiqui, A. A. Al-warthan and Wolfgang Tremel, *J. Mater. Chem. A* 3 (2015) 18753.
5. S. Park and R. S. Ruoff, *Nat. Nanotechnol.*, 4 (2009) 217.
6. R. Bissessur and S. F. Scually, *Solid State Ion.*, 178 (2007) 877.
7. S. J. Guo and S. J. Dong, *Chem. Soc. Rev.*, 40 (2011) 2644.
8. D. Chen, L. H. Tang and J. H. Li, *Chem. Soc. Rev.*, 39 (2010) 3157.
9. A. J. Haque, H. Park, D. Sung, S. Jon, S. Cho and K. Kim, *Anal. Chem.*, 84 (2012) 1871.
10. Z. H. Shen, X. Q. Zheng, J. Y. Xu, W. J. Bao, F. B. Wang and X. H. Xia, *Biosens. Bioelectron.*, 34 (2012) 125.
11. D. Voet and J. G. Voet, *Biochemistry, II edn.*, Wiley, New York, 1995.
12. M. Salimi and Roushani, *Electroanal.*, 18 (2006) 2129.
13. T. Hoshi and S. H. Heinemann, *J. Physiol.*, 531 (2001) 1.
14. A. John Jeevagan and S. Abraham John, *Bioelectrochemistry*, 85 (2012) 50.
15. E. Zor, M. E. Saglam, S. Alpaydin and H. Bingol, *Anal. Methods.*, 6 (2014) 6522.
16. T. A. Enache and A. M. Oliveira-Brett, *Bioelectrochemistry*, 81 (2011) 46.
17. B. Paulchamy, G. Arthi and B. D. Lignesh, *Nanomedicine & Nanotechnology*, 6 (2015) 1.
18. J. Wu, X. Shen, L. Jiang, K. Wang and K. Chen, *Appl. Surf. Sci.*, 256 (2010) 2826.
19. X. M. Sun and Y. D. Li, *Angew. Chem. Int. Ed.*, 43 (2004) 597.
20. S. Tajik, M. A. Taher, H. Beitollahi, R. Hosseinzadeh and M. Ranjbar, *Electroanalysis*, 28 (2016) 656.
21. D. O. Perevezentseva, K. V. Skirdin, E. V. Gorchakov and V. I. Bimatov, *Key Eng. Mater.*, 685 (2016) 563.
22. M. E. Tess and J. A. Cox, *Electroanalysis*, 10 (1998) 1237.
23. L. Ozcan and Y. Sahin, *Sens. Actuators B* 127 (2007) 362.
24. N. D. Popovic and D. C. Johnson, *Electroanalysis*, 11 (1999) 934.
25. U. Satyanarayana and U. Chakrapani, *Biochemistry*, 3rd ed. (2007) pp. 43-55.
26. H. Xu, W. Zhang, W. Zhu, D. Wang, J. Ye, K. Yamamoto and L. Jin, *Anal. Chim. Acta.*, 545 (2005) 182.
27. J. A. Dean, *Lange's Handbook of Chemistry*, McGraw-Hill, New York 1973.
28. S. B. Revin and S. A. John, *Electrochim. Acta*, 56 (2011) 8934.
29. O. Daniel and Br. J. Urol. *BJU Int.*, 26 (1954) 153.
30. P. Kalimuthu and S. A. John, *Electrochem. Commun.*, 11 (2009) 367.
31. J. G. Velasco, *Electroanalysis*, 9 (1997) 880.
32. P. Kalimuthu and S. A. John, *Electrochim. Acta*, 55 (2009) 183.